Interdependent lateral interactions, hydrophobicity and acid strength and their influence on the catalytic activity of nanoporous sulfonic acid silicas†

Jean-Philippe Dacquin,[a] Hannah E. Cross,[b] D. Robert Brown,[b] Tina Düren,[c] Jennifer J. Williams,[c] Adam F. Lee[a] and Karen Wilson*[a]

Received 26th April 2010, Accepted 8th June 2010
First published as an Advance Article on the web 13th July 2010
DOI: 10.1039/c0gc00045k

A series of propylsulfonic (MCM–SO_3H) and octyl co-functionalised propylsulfonic (MCM–Oc–SO_3H) catalysts have been prepared by post modification of MCM-41 with mercaptopropyltrimethoxysilane (MPTS) to achieve SO_3H surface coverages spanning the range 0.12–1 monolayer. Within the MCM–Oc–SO_3H series, samples with submonolayer MPTS coverages were further grafted with octyltrimethoxysilane to cap bare hydroxyl sites and tune the hydrophobicity of the support. For the MCM–SO_3H series NH_3 calorimetry revealed acid strength increases as a function of sulfonic acid loading, with $-\Delta H_{ads}(NH_3)$ increasing from 87 to 118 kJ mol^{-1}. In contrast, MCM–Oc–SO_3H exhibits a dramatic enhancement of acid strength for submonolayer SO_3H coverages, with $-\Delta H_{ads}(NH_3)$ found to increase to 103 kJ mol^{-1}. In line with these acid strength measurements the per-site activity of the MCM–SO_3H series in the esterification of butanol with acetic acid was found to increase with SO_3H content. Incorporation of octyl groups further promotes esterification activity of all the samples within the MCM–Oc–SO_3H series, such that the turn over frequency of the sample with the lowest loading of SO_3H more than doubles. Molecular dynamic simulations indicate that the interaction of isolated sulfonic acid groups with the pore walls is the primary cause of the decrease in acid strength and activity of submonolayer samples within the MCM–SO_3H series. Incorporation of octyl groups results in a combination of increased hydrophobicity and lateral interactions between adjacent sulfonic acid head groups, resulting in a striking enhancement of acid strength and esterification activity.

1. Introduction

Many fine and speciality chemicals manufacturers, who rely on homogeneously catalysed processes[1] resulting in the production of vast quantities of waste and toxic emissions, are seeking cleaner heterogeneous alternatives to meet ever tightening legislation.[2] The development of new catalytic routes for the manufacture of fine, speciality and pharmaceutical chemicals is one of the principal solutions for addressing the sustainability and environmental impact of chemical processes. Acid initiated reactions are widely used in, for example, alkylation, acylation, esterification, and isomerisation reactions, and are a major area in which new catalyst systems are required.

The discovery of structured mesoporous materials with high surface areas and large regular pore frameworks over the range of 2–10 nm[3–5] has stimulated much interest in their application as catalyst supports. Facile organic modification of these materials[6] *via* a range of functional silanes generates derivatised nanomaterials containing phenyl, cyano, vinyl, amine, thiol, carboxylic acid or sulfonic acid groups.[7–10] The synthesis of sulfonic acid functionalised mesoporous silicas[11–15] has stimulated significant research efforts in this area and been the subject of recent reviews,[16,17] since they are interesting alternatives to commercially available sulfonated polymer resins, such as Amberlyst-15 and Nafion-H, which suffer from low surface areas and thermal stability.[18–20] The development of next generation catalyst materials however requires improved understanding of how the acid site distribution and surface functionality affects in-pore diffusion and adsorption processes.

The design of heterogeneous catalysts with tuneable acidity and surface polarity is an ultimate goal in the development of solid acid catalysts. Such properties are the key for controlling adsorption properties, reactant activation and product selectivity in vapour and liquid phase catalysis. Despite the interest in the catalytic applications of sulfonic acid silicas, two fundamental questions concerning their application in liquid phase reactions remain unclear. First, does the packing density of sulfonic acid groups on the silica surface affect the overall acidity? Second, can the polarity of the silica surface be controlled to alter the diffusion and adsorption of hydrophobic organic reactants?

Recent investigations have set out to address these issues through the use of designer sulfonic acid precursors which offer control over the spatial location of acid centres, and by

[a]*Cardiff Catalysis Institute, School of Chemistry, Cardiff University, Cardiff, CF10 3AT, UK. E-mail: WilsonK5@cardiff.ac.uk, Leeaf@cardiff.ac.uk; Fax: +44 29208 74030; Tel: +44 29208 70827*
[b]*Department of Chemical and Biological Sciences, University of Huddersfield, Huddersfield, HD1 3DH, UK. E-mail: D.R.Brown@hud.ac.uk*
[c]*Institute for Materials and Processes, School of Engineering, The University of Edinburgh, Edinburgh, EH9 3JL. E-mail: Tina.Duren@ed.ac.uk*

† Electronic Supplementary Information (ESI) available: MCM characterisation, esterification profiles, simulation details and link to movies. See DOI:10.1039/c0gc00045k/

incorporation of inert organic groups to alter the hydrophobicity of the surface. The use of disulfide or sulfonate ester functionalities[21] to generate spatially located alkylsulfonic acid groups has been found to almost double the turn over frequency in bisphenol-A synthesis. However, incomplete conversion of the precursor to the sulfonic acid meant it was unclear whether this enhancement reflected residual S–H or S–S present in the catalysts. Similar studies on fatty acid esterification[22] using a bis(trimethoxysilyl)propyl disulfide precursor to functionalise SBA-15 revealed an increase in acid strength for the resulting spatially located sulfonic acid groups, but could not subsequently correlate these observations with catalytic activities. SBA-15 propyl sulfonic acids co-functionalised with methyl, ethyl and phenyl groups have also been investigated in fatty acid esterification to determine whether tuning the surface hydrophobicity can increase catalytic activity.[23] While some differences in initial rates of reaction were reported, the textural properties of SBA-15 also varied across the series making it difficult to draw firm conclusions about the effect of apolar spectator groups.

To address these issues, herein we report a combined experimental and computational study of a series of sulfonic acid functionalised MCM-41 materials in which special attention has been paid to the effect of acid site density on the overall acidity and catalytic performance. MCM-41 was selected as the support due to the availability of accurate models for the pore structure generated using kinetic Monte Carlo simulations.[24] This MCM-41 pore model can also be readily modified with surface groups thus allowing dynamic simulation of sulfonic acid and octyl groups attached within the MCM pores. Two series of catalysts are investigated in which the propylsulfonic acid coverage was varied over the range $\theta(RSO_3H) = 0$–100% ML (MCM–SO_3H), and an octyl co-grafted series with octyl coverage varies as 100-$\theta(RSO_3H)$ (MCM–Oc–SO_3H) as illustrated in Scheme 1. To ensure there are no complications in the kinetic analysis from diffusion limitation, esterification of a short chain alcohol, butanol, with acetic acid has been selected as a model reaction. In particular we focus on understanding the effect of lateral interactions between propylsulfonic acid heads groups and the role of inert hydrophobic octyl chain 'spectator groups' on acid strength and catalyst activity.

2. Experimental

Two series of pure sulfonic and octyl co-functionalised sulfonic acid catalysts were prepared. The monolayer coverage of thiol was determined by grafting from a solution containing a three fold excess of thiol (based on hydroxyl content) which is referred to MCM–SO_3H-ovs. The saturated monolayer thiol coverage was then used to determine the quantities required for the preparation of grafted silicas with coverages of $\theta = 25$, 50, 75 and 100% of the saturation monolayer. The final materials are respectively termed MCM–SO_3H-θ and MCM–Oc–SO_3H-θ.

2.1 MCM-41 synthesis

The mesoporous organized material was prepared according to a surfactant template method reported by Grün *et al.*,[25] to yield a long range ordered framework with highly uniform mesopores.

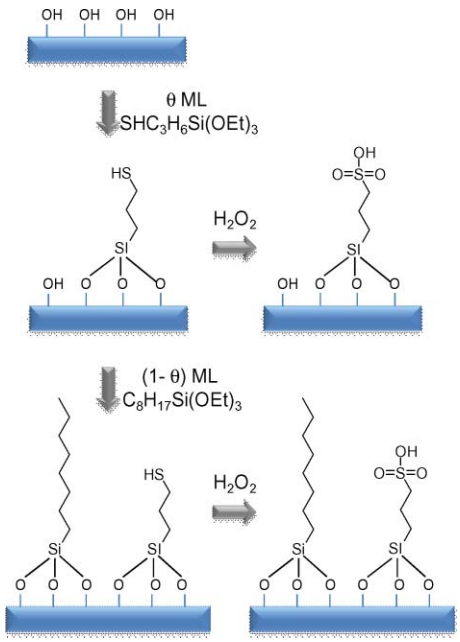

Scheme 1 Preparation of sulfonic acid and octyl co-functionalised sulfonic acid MCM-41 materials.

The mesoporous silica phase was synthesised at room temperature by using a cationic surfactant as the structure-directing agent. All the samples originate from the same silica batch. In a typical preparation, 25 g of n-hexadecyltrimethylammonium bromide (C_{16}TMABr) was dissolved in 500 mL of deionised water and 132 g of aqueous ammonia (32 wt%), with 760 mL of absolute ethanol added to the surfactant solution under stirring conditions (250 rpm). After 30 min, 47 g of tetraethoxyorthosilicate (TEOS) was added, resulting in a gel, and the solution was constantly stirred for four hours. After filtration and washing with water followed by methanol, the precipitate was dried overnight at 80 °C and calcined under air at 550 °C (1 °C min^{-1} for a duration of 5 h).

2.2. MCM sulfonic acid (MCM–SO_3H)

A large range of propyl-sulfonic acid-functionalised silicas were first prepared by a post-synthesis grafting method[26] utilising the following procedure. After a drying step of 3 h at 110 °C, 1 g of calcined MCM-41 was heated in 15 mL of toluene at 130 °C under vigorous stirring within a three-necked round bottom flask. Then, the addition of the required amount of MPTS (3-mercaptopropyltrimethoxysilane) per gram of solid was added ($0.04 < MPTS/MCM\text{-}41 < 1.00$). The solution was refluxed for 24 h and the resulting functionalised silica was then isolated by filtration and intensively washed with methanol before being dried overnight at 80 °C. Subsequent oxidation of the propylthiol groups was carried out at room temperature with H_2O_2 for 24 h (20 mL of 33 wt% H_2O_2 per gram of material). Finally, successive filtration and intensive washings with methanol were performed and the final materials were dried at 80 °C.

2.3. Octyl grafted MCM sulfonic acid (MCM–Oc–SO_3H)

The octyl grafted materials were obtained by reaction of the un-oxidised thiol functionalised silicas (mentioned above, with theoretical 25, 50, 75 and 100 % ML loadings), with an excess of octyltriethoxysilane. Typically, 1 g of the un-oxidised thiol grafted sample was refluxed for 24 h at 130 °C in 15 mL toluene with 3 mmol of octyltriethoxysilane. The co-grafted samples were isolated and dried as mentioned above. Propylthiol groups were finally oxidised using a peroxide solution for 24 h (20 mL of 33 wt% H_2O_2 per gram of material). Following filtration and intensive washing with methanol the final materials were dried at 80 °C.

2.4 Material characterisation

Powder X-ray diffraction patterns were collected on a Bruker D8 advanced X-Ray diffractometer fitted with a Lynx eye high-speed strip detector and a Cu-Kα radiation source. Small-angle X-ray diffraction patterns were acquired from 0.3° to 6° with a 0.02° step size. Nitrogen porosimetry was performed on a Quantasorb Nova 1200 instrument, after treatment of the samples under vacuum at 200 °C for 4 h. Surface areas were calculated using the Brunauer Emmet Teller (BET) method over the range P/P0 = 0.07–0.30, where a linear relationship was maintained. Pore size distributions were calculated using the Barrett-Joyner-Halenda (BJH) model applied to the desorption branch of the isotherm. Mesopore volume was evaluated on the volume adsorbed at P/P0 = 0.98.

Thermogravimetric analyses were performed using a Stanton Redcroft STA 780 thermal analyser. Samples were mounted in an alumina crucible and heated at a rate of 5 °C min^{-1} to 800 °C under flowing 20 vol% O_2/He gas (20 ml min^{-1}). Sulfur content was determined using an Horiba XGT-7000 X-Ray Fluorescence spectrometer. XRF can only detect elements greater than Na in the periodic table, thus atomic compositions employ manufacturer's elemental response factors for S and Si and use an algorithm which assumes Si is present in a non-porous SiO_2 matrix. XPS measurements were performed using a Kratos AXIS HSi instrument equipped with a charge neutraliser and Mg X-ray source. Material functionality was investigated by diffuse reflectance infrared Fourier transform spectroscopy (DRIFT) using a Thermo Nicolet Avatar 370 MTC. Samples were prepared by grinding 20 mg of sample with 330 mg of dried KBr.

Ammonia adsorption calorimetry under flow conditions was performed using a system based on a flow-through Setaram 111 differential scanning calorimeter (DSC) and an automated gas flow and switching system, with down-stream mass spectrometer detector (Hiden HPR20) connected *via* a heated capillary. In a typical experiment, the sample (5–15 mg) was activated under dried helium (5 ml min^{-1}) for 2 h at 100 °C. Adsorption was monitored at 100 °C, so measured enthalpies correspond only to ammonia that binds irreversibly to the catalyst at this temperature. Small pulses (typically 1 mL) of the probe gas (1% ammonia in helium) were then injected at regular intervals into the carrier gas stream from a gas sampling valve, also at 100 °C. The concentration of ammonia down-stream of the sample was monitored with the mass spectrometer ($m/z = 15$), and heat evolution with the calorimeter. The net amount of ammonia irreversibly adsorbed from each pulse was determined by comparing the mass spectrometer signal during each pulse with a signal recorded through a blank sample tube during a control experiment. Net heat released for each pulse was calculated from the DSC thermal curve. From this the molar enthalpy of ammonia adsorption $\Delta H°$ Ads NH_3 was obtained for the ammonia adsorbed from each pulse. Each sample was analysed in duplicate under the same experimental conditions. Data was plotted as a profile of $\Delta H°$ Ads NH_3 *vs.* amount of ammonia irreversibly adsorbed.

2.5 Catalyst testing

Esterification of acetic acid was performed at 60 °C under stirring using 0.05 g of catalyst, 2.402 g (40 mmol) of acetic acid, 0.742 g of butan-1-ol (10 mmol) and 0.6 g (3.2 mmol) of dihexylether as internal standard. Aliquots of 0.1 mL were regularly sampled and analyzed using a Varian 3900 GC equipped with a CP-Sil 5CB, 15 m × 0.25 mm capillary column. Product yields were calculated using response factors derived for butyl acetate.

2.6 Molecular dynamics

For molecular simulations, the pore structure of MCM-41 was created using a kinetic Monte Carlo (kMC) method.[24] The resulting unit cell was a 3D periodic parallelepiped box with dimensions $a = 46.4207$ Å, $b = 43.6299$ Å, $c = 18.9596$ Å, $\alpha = \beta = 90°$ and $\gamma = 120°$. A Monte Carlo (MC) optimisation scheme[27,28] was used to functionalize the pore walls with surface group concentrations corresponding to those in the real material. The surface group functionalization is carried out by replacing the required number of silanol (OH) groups with propylsulfonic acid/octyl functional groups. Initially the silanol groups to be substituted are chosen randomly. Then, to generate a more realistic distribution of surface groups the positions of the surface groups and unfunctionalized silanol groups are swapped. The swapping of groups is continued until the energy reaches a local minimum. At this point, surface groups are bound to the surface in a position where they can assume a configuration of low strain, and the models obtained feature a random configuration of surface groups with a reasonably low potential energy.

To investigate the interaction of surface groups, molecular dynamics simulations were carried out using Gromacs v. 4.0.7[29] in the NVT ensemble at 300 K controlled using the Nose-Hoover thermostat[30] with a time step of 1 fs. Simulations were typically carried out over 5 ns with 10% of the total simulation time being allowed for equilibration. Positions, velocities and forces were written to disk every 1000 steps and used to generate movies. Full details of the potential parameters used in the simulation are given in section 3 of the supporting information†.

3. Results and discussion

3.1. Material characterisation

The structural and textural properties of the parent MCM material was first assessed by XRD and N_2 porosimetry (figure

Table 1 Surface and bulk sulfur content of MCM–RSO_3H-θ and MCM–Oc–RSO_3H-θ catalyst series[c]

Samples[a]	Bulk S content/ mmol g^{-1}	Surface S content/ mmol g^{-1}	Sulfur[b] density/ nm^{-2}	Total NH_3 ads/ mmol g^{-1}	Average[c] $-\Delta H°_{ads}(NH_3)$/ kJ mol^{-1}
MCM-SO_3H-25	0.15	0.09	0.09	0.08	87
MCM-SO_3H-50	0.22	0.13	0.14	/	/
MCM-SO_3H-75	0.27	0.16	0.19	0.12	94
MCM-SO_3H-100	0.49	0.21	0.37	0.19	99
MCM-SO_3H-ovs	0.58	0.28	0.47	0.24	118
MCM-Oc-SO_3H-25	0.07	0.05	0.05	0.06	103
MCM-Oc-SO_3H-50	0.13	0.07	0.09	/	110
MCM-Oc-SO_3H-100	0.52	0.10	0.34	/	113
MCM-Oc-SO_3H-ovs	0.58	0.11	0.37	0.15	115

[a] Nominal surface coverage (θ) defined as % of saturation monolayer of RSO_3H. [b] Calculated from bulk S loading - full compositional analysis shown in table S2a-b. [c] Average of molar enthalpies of all pulses of NH_3 that adsorbed with enthalpies greater than 80 kJ mol^{-1}.

S1†) which revealed the support to have a narrow pore diameter of 2.5 nm and a high specific surface area of 1044 m^2g^{-1}. Such properties are appropriate for incorporation of propylsulfonic groups (RSO_3H) without pore blockage and these parameters were used to create the pore model for molecular simulations in section 3.4. The surface silanol density was estimated from TGA (figure S2) to be ~ 0.78 ± 0.05 mmol g^{-1}, corresponding to a surface density of 0.45 ± 0.03 OH nm^{-2}, which provides a measure of the expected saturation RSO_3H coverage, and is consistent with values reported in literature.[31,32]

Successful grafting of mercaptopropyl thiol groups on both series and their subsequent oxidation to yield tethered sulfonic acid centres, was subsequently assessed *via* XRF, XPS, DRIFT and NH_3 calorimetry. A progressive increase in both surface and bulk sulfur content is obtained for both series (Table 1) with final surface densities ~ 0.5 RSO_3H nm^{-2} typical for grafted sulfonic acid silicas.[33,15] XRD and porosimetry confirm that the structural integrity of MCM is retained following both oxidation to RSO_3H and grafting of octyl groups (table S1, figure S3†). Furthermore, no residual unoxidised S is observed by XPS, with a single S chemical environment with a binding energy of 169.9 eV present upon hydrogen peroxide treatment, indicative of complete thiol oxidation to sulfonic acid (figure S4). Overall these results demonstrate that a wide range of SO_3H loadings have been achieved spanning submonolayer to monolayer coverages for both series.

The successful incorporation of the octyl spectator groups in the co-functionalised series was subsequently investigated by XPS and DRIFTS. Fig. 1 shows how the surface sulfonic acid and octyl group loadings, determined from XPS, varies for the MCM–Oc–SO_3H-θ series as a function of bulk S content. These results clearly demonstrate a systematic variation in surface compositions across the series, with samples with low initial S content found to be co-functionalised with the highest coverage of octyl groups. This is in line with the expected functionalisation of free silanols by $C_8H_{17}Si(OEt)_3$ at low RSO_3H coverages, with increased θ (RSO_3H) leading to proportionally fewer free sites for octyl attachment.

Subsequent DRIFT analysis, shown in Fig. 2 for the θ = 25 series, also confirms an increase in alkyl functionality upon grafting octyl groups. The bare support is characterised by a broad envelope centred at 3350 cm^{-1}, a shoulder at 3640 cm^{-1} and a sharp band at 3748 cm^{-1} which are assigned respectively

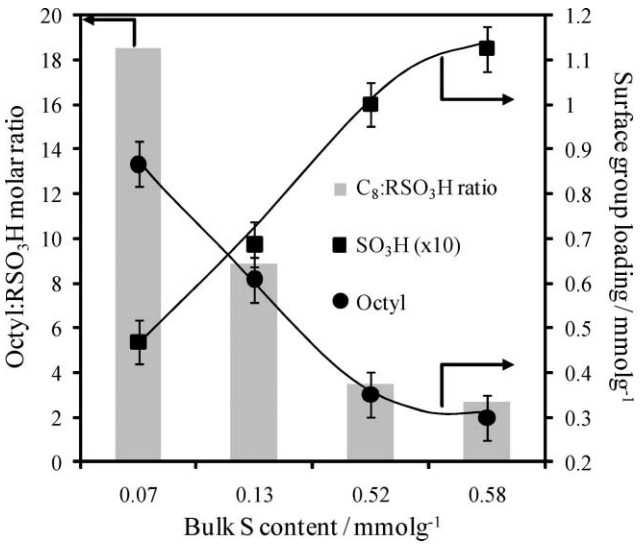

Fig. 1 Surface loadings of sulfonic acid and octyl groups as determined by XPS for the MCM–Oc–SO_3H-θ series.

to physisorbed water along with vicinal and isolated hydroxyl groups.[34,35] Following grafting with RSO_3H the latter features are attenuated, suggesting covalent anchoring of surface groups to the free hydroxyls. The existence of such octyl-surface groups is evidenced by asymmetric and symmetric C–H stretching vibrations between 2930 and 2871 cm^{-1} as highlighted in spectrum (c). The strongest intensity of these bands is due to the large number of -CH_2 groups in the octyl-modified silica compared to the pure propylsulfonic sample. In addition, a slight decrease in the surface-adsorbed water intensities centred at 3450 and 1635 cm^{-1} (not shown) suggests an increase in the hydrophobicity of the octyl-grafted materials.

Ammonia adsorption calorimetry was performed to probe the acid strength of the grafted materials (Table 1). The concentration of acid sites measured by ammonia adsorption is taken as the amount of ammonia adsorbed up to the point where $\Delta H°_{ads}(NH_3)$ falls numerically below 80 kJ mol^{-1}, on the basis that enthalpies less than 80 kJ mol^{-1} are not significantly acidic.[36,37] The number of acid sites determined from the total volume of NH_3 adsorbed is in broad agreement with the surface S coverage from XPS, corroborating that all the observed S is present as SO_3H. Fig. 3 shows how the acid strength of both

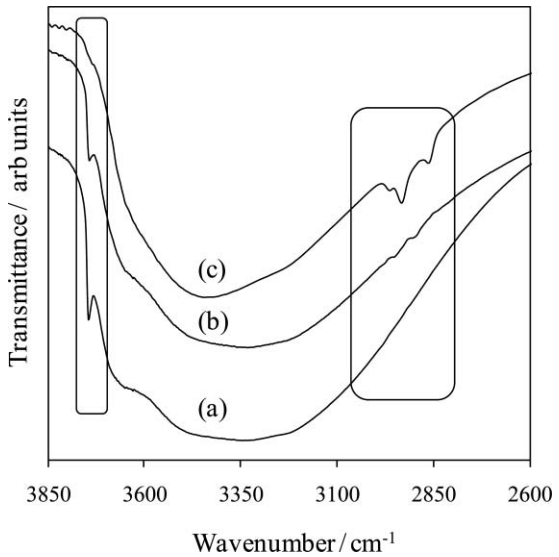

Fig. 2 DRIFT spectra of (a) MCM-41, (b) MCM–SO_3H-25, (c) MCM–Oc–SO_3H-25.

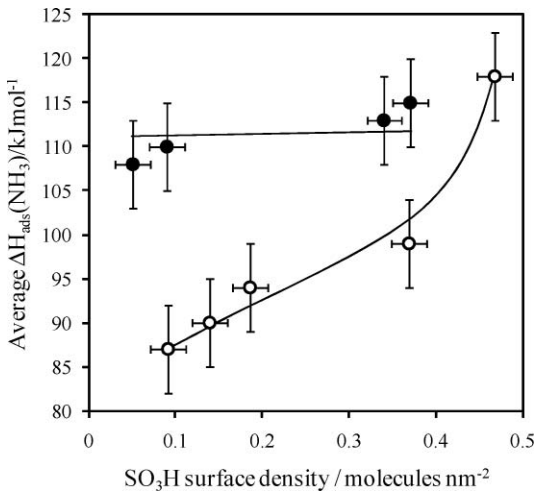

Fig. 3 Variation in acid strength with surface RSO_3H density for (○) MCM–SO_3H-θ and (●) MCM–Oc–SO_3H-θ materials.

MCM–SO_3H-θ and MCM–Oc–SO_3H-θ materials varies as a function of acid site density.

The first thing to note is that for the MCM–SO_3H series, the acid strength (measured as molar enthalpies of ammonia adsorbed) increases with SO_3H surface density. This is in line with ^1H NMR measurements on co-condensed SBA–RSO_3H materials with S loadings 2–10 wt%[38] prepared *via* a one-pot approach and calorimetric measurements on sulfonated polystyrene resins.[39] However, a remarkable enhancement of acid strength is observed for the lowest loading MCM–Oc–SO_3H-θ samples (*i.e.* those with the most octyl functionality), with $\Delta H_{ads}(NH_3)$ found to be almost invariant across the series, with a value close to that for MCM–SO_3H_{ovs}. These observations suggest that the nature of the acid sites is changed in the presence of octyl groups, which may originate from a reduction in acid site solvation by physisorbed water,[40] or a change in the lateral interactions between sulfonic acid head groups. The increased hydrophobic character on incorporation of octyl groups will reduce surface H_2O adsorption and increase the H^+ activity of the sulfonic acid headgroups. Calorimetric studies on analogous sulfonated polystyrene resins reveal that the average acid strength increases with degree of sulfation for both hydrated and anhydrous resins.[41] In the anhydrous state, acid strength is linked to interactions between headgroups, while in the hydrated state it is linked to local concentration of acid sites within the pores. The origin of this increase in acid strength for sulfonic acid silicas will be discussed in the context of the molecular simulations in section 3.4.

3.3 Catalytic reactivity

Catalyst activity of the series of MCM–SO_3H and MCM–Oc–SO_3H materials was subsequently assessed in the esterification of butanol with acetic acid (Scheme 2) at 60 °C.

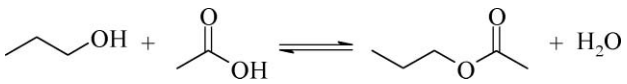

Scheme 2 Esterification of butanol with acetic acid.

The resulting reaction profiles (reported in figures S5a and b†) were used to calculate the turn over frequencies (TOFs) shown in Fig. 4 as a function of surface SO_3H density. For the MCM–SO_3H series it is immediately evident that increasing the surface density of acid sites results in an enhancement of the overall catalytic activity. This increase is in line with the calorimetry measurements which suggest the acid strength increases with SO_3H density, with stronger acid sites expected to exhibit higher activity in esterification reactions.[42]

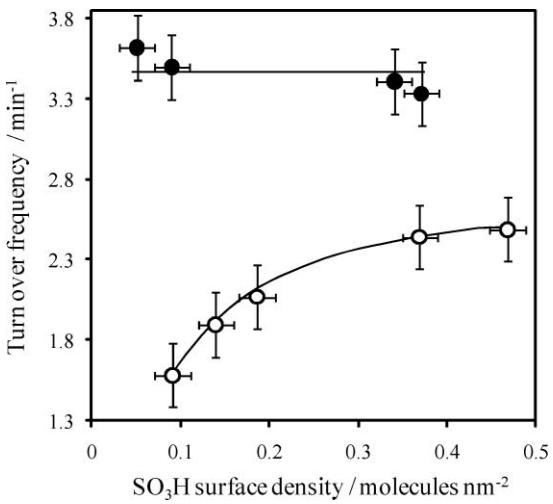

Fig. 4 Effect of SO_3H surface density on turn over frequency in butanol esterification. (○) MCM–SO_3H, (●) MCM–Oc–SO_3H.

The effect of octyl spectator groups in the MCM–Oc–SO_3H series also has a striking effect on the TOF, with the per site activity of the lowest loading of catalyst found to be more than doubled. Activity is found to be almost constant as a function of surface SO_3H density upon octyl co-functionalisation, which is in line with the observations that acid strength is almost invariant across the MCM–Oc–SO_3H series. The differences in activity for the two series cannot however be accounted for by acid strength alone, as calorimetry measurements indicate that the strength of

the highest loading catalysts from the two series are comparable. Thus the effect of increased hydrophobicity of the MCM–Oc–SO_3H series is also expected to contribute to the enhanced TOF in this instance. To investigate this, the effect of addition of 2.5 mmol of H_2O on the esterification rate was studied (Figure S6†), which revealed the TOF for MCM–SO_3H-25 had decreased by >50%. In contrast MCM–Oc–SO_3H-25 was found to only lose around a third of its per-site activity, indicating that octyl groups influence water adsorption at the active site. Such effects of water can be understood in terms of esterification being an equilibrium reaction. The rate of esterification will be dependent on the local H_2O concentration near the acid site and thus the reverse hydrolysis reaction,[43] which in turn will be dependent on the hydrophobicity of the catalyst. Indeed it is demonstrated that as water is produced during esterification of methanol with acetic acid,[44] deactivation of liquid H_2SO_4 catalysts can be observed. On solid acid catalysts, competitive adsorption of water and alcohol at the acid site also leads to loss of catalyst activity. Increased hydrophobicity can help reduce the sticking probability of water and thus its impact on catalyst activity. Such effects have been illustrated by the use of organosilica based sulfonic acids which exhibit enhanced activity in butanol dehydration.[45]

The effect of water adsorption on the kinetics may also explain the asymptote in the TOF observed for the stronger acids in the MCM–SO_3H series. Recent studies of phenyl sulfonic acid SBA materials have shown that despite being stronger acids than the propyl variant, these are actually less active in etherification, where again water is generated as by-product. These observations were attributed to stronger acids being more hydrophilic,[46] leading to enhanced local H_2O adsorption and exhibiting lower catalyst activity, and are in line with our observations for the MCM–SO_3H series.

The trend in TOFs for the two catalyst series also provides an important insight into the location of sulfonic acid groups within the MCM support. Previous work using vinyl[47] and propylamine[48] functionalised silanes have inferred that preferential grafting of alkoxy silanes occurs at external Si–OH sites. Considering the two series of materials in this study, if RSO_3H groups are preferentially located at the external surface, then the diffusional barriers to reaction would be small, resulting in a high initial TOF for the samples with lower loadings. Increased in-pore grafting at higher coverages would then lead to a decrease in the TOF due to the effect of in-pore diffusional limitations. This is precisely the opposite to the observations in this study suggesting that for MCM–RSO_3H a uniform distribution of groups throughout the pore network can be achieved.

3.4 Molecular dynamic simulation

To understand the origin of the effect of RSO_3H loading and octyl co-functionalisation on acid strength, molecular simulations were performed. Initially a kinetic Monte Carlo (kMC) method to create pore structures (Figure S7†),[24] and a Monte Carlo (MC) optimisation scheme[27,28] was used to functionalize the pore walls with surface groups. Molecular dynamics simulations were then carried out to assess the interaction of surface groups with each other and the MCM-41 pore wall. Samples from the MCM–SO_3H series with loadings of 0.58 and 0.15 mmol g^{-1} were first simulated to investigate the effect of surface density on SO_3H head group orientation and lateral interactions. The effect of octyl groups on the 0.15 mmol g^{-1} sample was also studied following further functionalisation of this model with 0.43 mmol g^{-1} of octyl groups. Scheme 3a shows a representative snapshot of the 0.15 mmol g^{-1} model, in which three surface RSO_3H groups can be seen, in which sites (1) and (2) are in close proximity, whereas site (3) is isolated. All three materials were constructed so these three surface groups were in common and allowed a comparison of the effect of further functionalization on the orientation of these three groups.

The arrangement in the MCM-41 material functionalized with 0.15 mmol g^{-1} $C_3H_7SO_3H$ presents an opportunity to assess the extent of interaction between neighbouring propylsulfonic acid groups. In this structure, one of the propylsulfonic acid groups (3) is isolated and too far away from other surface groups to interact to any significant extent. The other two surface groups (1) and (2) are in close proximity allowing lateral interactions to be probed. Scheme 3a shows that the polar SO_3H head groups of the isolated propylsulfonic acid (3) has a tendency to interact with the surface silanol groups of the pore wall. In order to express in a quantitative manner, the degree to which the surface groups interact with the pore wall, an angle φ was defined as the angle between the normal to the pore wall and the molecular axis (figure S8†). φ is thus a measure of the orientation of the surface group with respect to the pore wall which in turn is linked to the strength of the interaction between the pore wall and the surface group. A group which shows little interaction with the pore wall (*i.e.* is oriented towards the pore centre) will have a small φ, whereas φ will be large for a group which interacts strongly with the pore wall.

The orientation of the surface groups was analysed during a 4.5 ns simulation (figures S9-11†), which revealed that for isolated group (3), φ spans much larger angles and has a larger mean value than groups (1) or (2) indicating a stronger interaction with the pore wall. From the time resolved images, the group is seen to interact strongly with surface hydroxyl groups present in a niche of the pore wall. However, when other propylsulfonic acid surface groups are close enough as is the case with groups (1) and (2), interaction between the terminal oxygen and OH of SO_3H occurs. Scheme 3b shows the interaction of SO_3H groups becomes more significant as surface loading increases. For groups (1) and (2) which are close enough together to interact, φ is smaller. These surface groups spend much of the time in an approximately vertical position which facilitates the interaction of their terminal head groups in preference to the pore surface. Capping of adjacent silanol groups with octyl functionality (Scheme 3c) inhibits interaction of the SO_3H headgroup with the pore wall, forcing the propyl sulfonic acid groups into a more vertical geometry.

The effect of sulfonic acid surface density on acid strength can thus be understood in terms of these simulations, with surface group spacing determining their orientation and degree of lateral interactions. Sulfonic acid groups in very close proximity will interact only marginally with the pore wall as it is energetically favourable to interact with more polar neighbouring sulfonic acid groups. The tendency of these groups to interact with each other increases with their surface density, as the chain species

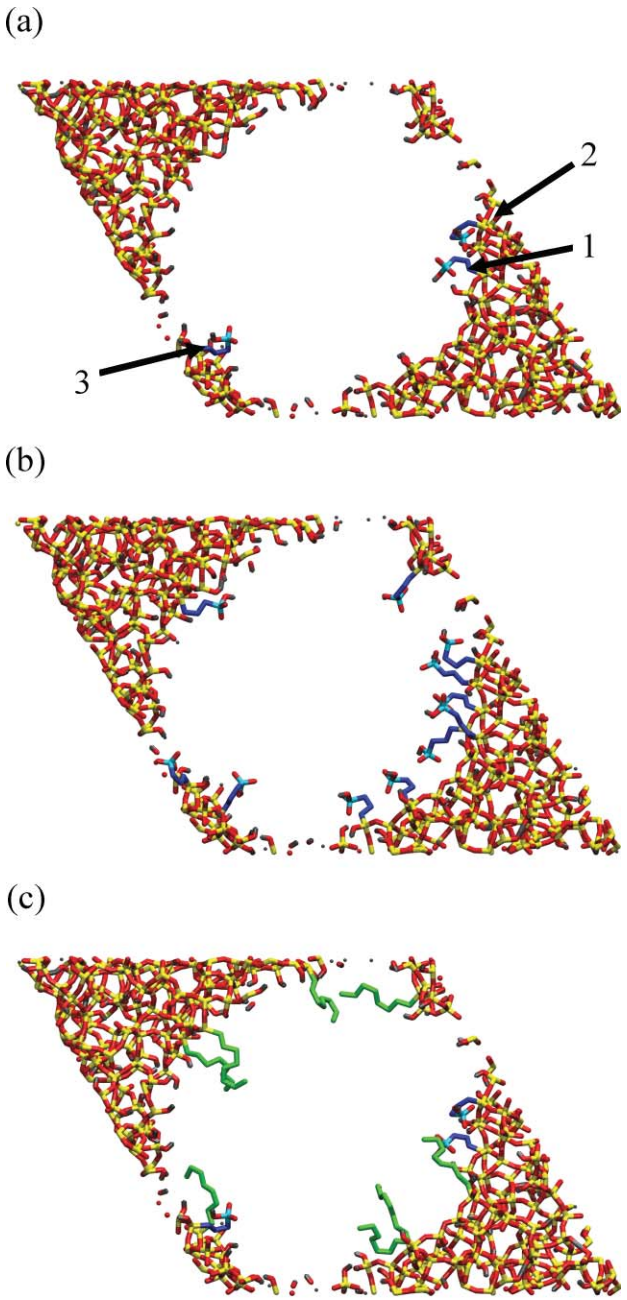

Scheme 3 Pore model for (a) 0.15 mmol g^{-1} MCM–RSO3H; (b) 0.58 mmol g^{-1} MCM–RSO3H and (c) 0.15 mmol g^{-1} MCM–RSO3H post functionalised with 0.43 mmol g^{-1} octyl groups. (Key: Si: yellow, O: red, H: grey, C of octyl group: green, S: light blue, C of sulfonic acid group: dark blue. Close up images of surface groups and movies showing movement of groups is available in the ESI).

will bend and twist so as to minimize the separation between neighbouring terminal groups.

It may be expected that the acid strength of sulfonic acid groups at the periphery of functionalised islands may be reduced as these have a higher likelihood of interacting with surface silanol sites. However, incorporation of octyl groups which cap free silanol groups prevents this interaction and thus increases the acid strength of these peripheral sulfonic acid sites.

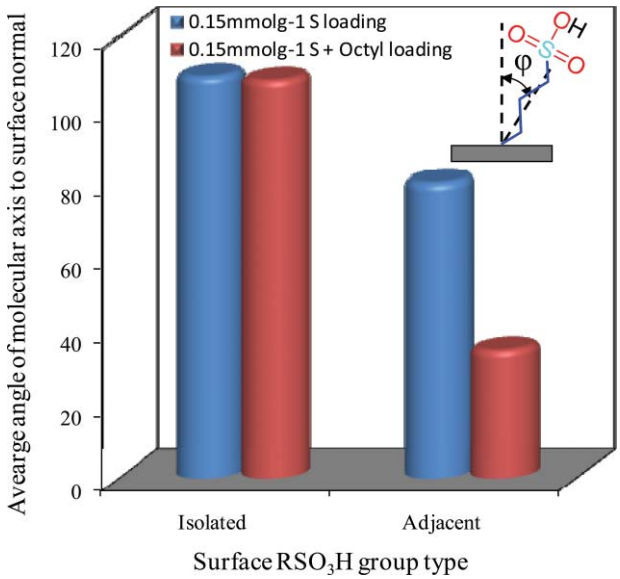

Fig. 5 Average orientation (φ) of surface functional groups. Isolated = surface group (3); adjacent = surface group (1); note that the amorphous nature of the simulated MCM-41 pore wall contains micro cavities and recesses giving rise to angles > 90°.

This effect of co-functionalisation with octyl groups can be seen most clearly by looking at the impact on the average orientation of surface group (1) which is adjacent to another sulfonic acid group and group (3) which is totally isolated (Fig. 5). Isolated groups which still have free hydroxyl groups in close proximity remain flat lying as hydrogen bonding to surface –OH dominates. However for SO_3H groups in a more confined environment (*e.g.* group (2)), binding of an adjacent octyl group decreases the average tilt angle and thus increases the degree of interaction between the neighbouring sulfonic acid site. This would correlate with an increase in acid strength and catalyst activity due to a cooperative effect between head groups. Such effects have been discussed in the context of sulfonated resins where a high density of adjacent acid sites is thought to increase alcohol activation *via* hydrogen bonding of the alcohol at one site and activation at the adjacent group.[49] Thus by capping free surface hydroxyls with octyl chains, the acid strength of sulfonic acid groups can be increased by inhibiting their interaction with the surface and promoting lateral interactions between adjacent groups as illustrated in Scheme 4. Likewise increased sulfonic acid loadings also enhance lateral interactions and acid strength, however these materials are more hydrophilic and less effective at expelling H_2O from the acid centres during esterification leading to reduced catalyst activity.

Conclusions

A series of propylsulfonic (MCM–SO_3H) and octyl co-functionalised propylsulfonic (MCM–Oc–SO_3H) catalysts have been prepared with surface coverages spanning a range 0.12–1 ML of grafted SO_3H groups. Octyl groups were used to cap residual silanol groups within pores of submonolayer samples and tune the hydrophobicity of the support. NH_3 calorimetry revealed that acid strength increases as a function of sulfonic acid loading for the MCM–SO_3H series. This variation in

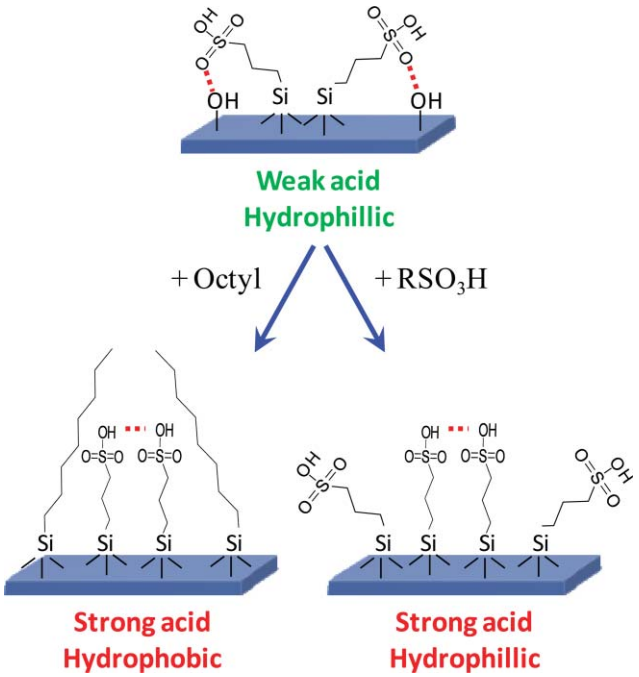

Scheme 4 Effect of octyl co-functionalisation and increasing sulfonic acid loading on lateral interactions and acid strength.

acid strength is attributed to a tendency of sulfonic acid head groups to interact with the pore walls at low coverages, with lateral interactions leading to increased acid strength at higher coverages. In contrast, for the MCM–Oc–SO_3H a dramatic enhancement of acid strength is observed for samples with submonolayer SO_3H coverages, with acid strength almost invariant of loading. Capping of free surface hydroxyls with octyl chains is proposed to increase acid strength of sulfonic acid groups by inhibiting their interaction with the surface and promoting lateral interactions between adjacent groups.

TOFs for the MCM–SO_3H series in butanol esterification were found to increase by ~66% as SO_3H content was increased which is in line with the acid strength increase. Incorporation of octyl groups further promotes activity of all the samples within the MCM–Oc–SO_3H series, such that the TOF of the lowest loading sulfonic acid sample more than doubled relative to its counterpart in the MCM–SO_3H series. From kinetic profiles and molecular simulations, it is proposed that upon incorporation of octyl groups a combination of increased hydrophobicity and lateral interactions between adjacent sulfonic acid head groups within the pore network are responsible for the striking enhancement of esterification activity.

Solvation effects may also play an important role in altering acid strength,[40] by moderating the chemical activity of H^+. Thus for MCM–SO_3H where physisorbed water may be appreciable, in-pore concentration effects may dictate overall acid strength. In contrast for the more hydrophobic MCM–Oc–SO_3H, a more anhydrous model may be envisaged where local interactions between acid groups are important. Sulfonic acid head groups interacting with the pore wall are also likely to be more sterically hindered than those free to move and oriented towards the centre of the pore. The enhanced interaction between adjacent head groups upon incorporation of octyl groups will not only have an important role to play in regulating acidity, but may also improve acid site accessibility. Future work will use molecular simulations to assess the effects of octyl co-functionalisation on preferred adsorption sites for butanol, acetic acid and water within the pores of sulfonic acid silicas.

Acknowledgements

We thank the Engineering and Physical Sciences Research Council for financial support (EP/E013090/1; EP/F063423/1; EP/G007594/1) and the award of a Leadership Fellowship (AFL).

Notes and references

1 R. A Sheldon, *Chemistry and Industry*, 1997, **12**.
2 P. T. Anastas, L. B. Bartlett, M. M. Kirchhoff and T. C. Williamson, *Catal. Today*, 2000, **55**, 11.
3 C. T. Kresge, M. E. Leonowicz, W. J. Roth, J. C. Vartuli and J. S. Beck, *Nature*, 1992, **359**, 710.
4 P. T. Tanev and T. J. Pinnavaia, *Science*, 1995, **267**, 865.
5 A. Corma, *Chem. Rev.*, 1997, **97**, 2373.
6 J. J. Pesek and M. T. Matyska, *Fundamentals and Applied Aspects of Chemically Modified Surfaces*, RSC, edited by J. P. Blitz and C. P. Little, 1999.
7 P. M. Price, J. H. Clark and D. J. Macquarrie, *J. Chem. Soc., Dalton Trans.*, 2000, 101.
8 A. Stein, B. J. Melde and R. C. Schroden, *Adv. Mater.*, 2000, **12**, 1403.
9 L. A. Ciolino and J. G. Dorsey, *J. Chromatography A*, 1994, **29**, 675.
10 L. Mercier and T. J. Pinnavaia, *Environ. Sci. Technol.*, 1998, **32**, 2749.
11 W. M. Van Rhijn, D. E. DeVos, B. F. Sels, W. D. Bossaert and P. A. Jacobs, *Chem. Commun.*, 1998, 317.
12 W. D. Bossaert, D. E. DeVos, W. M. VanRhijn, J. Bullen, P. J. Grobet and P. A. Jacobs, *J. Catal.*, 1999, **182**, 156.
13 I. Díaz, C. Marquez-Alvarez, F. Mohino, K. Prez-Pariente and E. Sastre, *J. Catal.*, 2000, **193**, 283.
14 D. Margolese, J. A. Melero, S. C. Christiansen, B. F. Chmelka and G. D. Stucky, *Chem. Mater.*, 2000, **12**, 2448.
15 J. A. Melero, G. D. Stucky, R. van Grieken and G. Morales, *J. Mater. Chem.*, 2002, **12**, 1664.
16 J. A. Melero, R. van Grieken and G. Morales, *Chem. Rev.*, 2006, **106**, 3790.
17 A. F. Lee and K. Wilson, 'Chapter 2: Sol–gel sulfonic acid silicas as catalysts' in *Handbook of Green Chemistry - Green Catalysis*, Edited by P. T. Anastas & R. H. Crabtree, Wiley-VCH, 2009, **2**.
18 M. A. Harmer, W. E. Farmeth and Q. Sun, *J. Am. Chem. Soc.*, 1996, **118**, 7708.
19 Q. Sun, M. A. Harmer and W. E. Farneth, *Chem. Commun.*, 1996, 1201.
20 M. A. Harmer, W. E. Farmeth and Q. Sun, *Adv. Mater.*, 1998, **10**, 1255.
21 V. Dufaud and M. E. Davis, *J. Am. Chem. Soc.*, 2003, **125**, 9403.
22 I. K. Mbaraka and B. H. Shanks, *J. Catal.*, 2006, **244**, 78.
23 I. K. Mbaraka and B. H. Shanks, *J. Catal.*, 2005, **229**, 365.
24 C. Schumacher, J. Gonzalez, P. Wright and N. Seaton, *J. Phys. Chem. B*, 2006, **110**, 319.
25 M. Grün, K. K. Unger, A. Matsumoto and K. Tsutsumi, *Microporous Mesoporous Mater.*, 1999, **27**, 207.
26 M. Boveri, J. Aguilar-Pliego, J. Perez-Pariente and E. Sastre, *Catal. Today*, 2005, **107–108**, 868.
27 C. Schumacher, J. Gonzalez, M. Perez-Mendoza, P. A. Wright and N. A. Seaton, *Stud. Surf. Sci. Catal.*, 2004, **154**, 386.
28 C. Schumacher and N. A. Seaton, *Adsorption-Journal of the International Adsorption Society*, 2005, **11**, 643.
29 B. Hess, C. Kutzner, D. van der Spoel and E. Lindahl, *J. Chem. Theory Comput.*, 2008, **4**, 435.
30 W. G. Hoover, *Phys. Rev. A: At., Mol., Opt. Phys.*, 1985, **31**, 1695.
31 X. S. Zhao, G. Q. Lu, A. K. Whittaker, G. J. Millar and H. Y. Zhu, *J. Phys. Chem. B*, 1997, **101**, 6525.
32 W. D. Bossaert, D. E. De Vos, W. M. Van Rhijn, J. Bullen, P. J. Grobet and P. A. Jacobs, *J. Catal.*, 1999, **182**, 156.

33 P. F. Siril, N. R. Shiju, D. R. Brown and K. Wilson, *Appl. Catal., A*, 2009, **364**, 95.
34 P. L. Llewellyn, F. Schuth, Y. Grillet, F. Rouquerol, J. Rouquerol and K. K. Unger, *Langmuir*, 1995, **11**, 574.
35 X. S. Zhao, G. Q. Lu, A. K. Whittaker, G. J. Millar and H. Y. Zhu, *J. Phys. Chem. B*, 1997, **101**, 6525.
36 M. J. Meziani, J. Zajac, D. J. Jones, S. Partyka, J. Roziere and A. Auroux, *Langmuir*, 2000, **16**, 2262.
37 A. Auroux, *Top. Catal.*, 1997, **4**, 71.
38 R. Kanthasamy, I. K. Mbaraka, B. H. Shanks and S. C. Larsen, *Appl. Magn. Reson.*, 2007, **32**, 513.
39 M. Hart, G. Fuller, D. R. Brown, J. A. Dale and S. Plant, *J. Mol. Catal. A: Chem.*, 2002, **182–183**, 439.
40 V. B. Kazansky, *Catal. Today*, 2002, **73**, 127.
41 M. Hart, G. Fuller, D. R. Brown, J. A. Dale and S. Plant, *J. Mol. Catal. A: Chem.*, 2002, **182–183**, 439.
42 X. Chen, Z. Xu and T. Okuhara, *Appl. Catal., A*, 1999, **180**, 261.
43 H. Liu, N. Xue, L. Peng, X. Guo, W. Ding and Y Chen, *Catal. Commun.*, 2009, **10**, 1734.
44 Y. Liu, E. Lotero and J. G. Goodwin Jr, *J. Mol. Catal. A: Chem.*, 2006, **245**, 132.
45 B. Sow, S. Hamoudi, M. Hassan Zahedi-Niaki and Serge Kaliaguin, *Microporous Mesoporous Mater.*, 2005, **79**, 129–136.
46 R. van Grieken, J. A. Melero and G. Morales, *J. Mol. Catal. A: Chem.*, 2006, **256**, 29.
47 M. H. Lim and A. Stein, *Chem. Mater.*, 1999, **11**, 3285.
48 D. S Shephard, W. Zhou, T. Maschmeyer, J. M. Matters, C. L. Roper, S. Parsons, B. F. G. Johnson and M. J. Duer, *Angew. Chem., Int. Ed.*, 1998, **37**, 2719.
49 B. C. Gates, J. S. Wisnouskas, H. W. Heath and Jr, *J. Catal.*, 1972, **24**, 320.